Development of a Portable Multispectral Aerial Sensor for Real-time Oil Spill Thickness Mapping in Coastal and Offshore Waters.

Final Report
Submitted to the U.S. Department of the Interior
Minerals Management Service
Herndon, VA

14 May, 2009

Contract No. M07PC13205

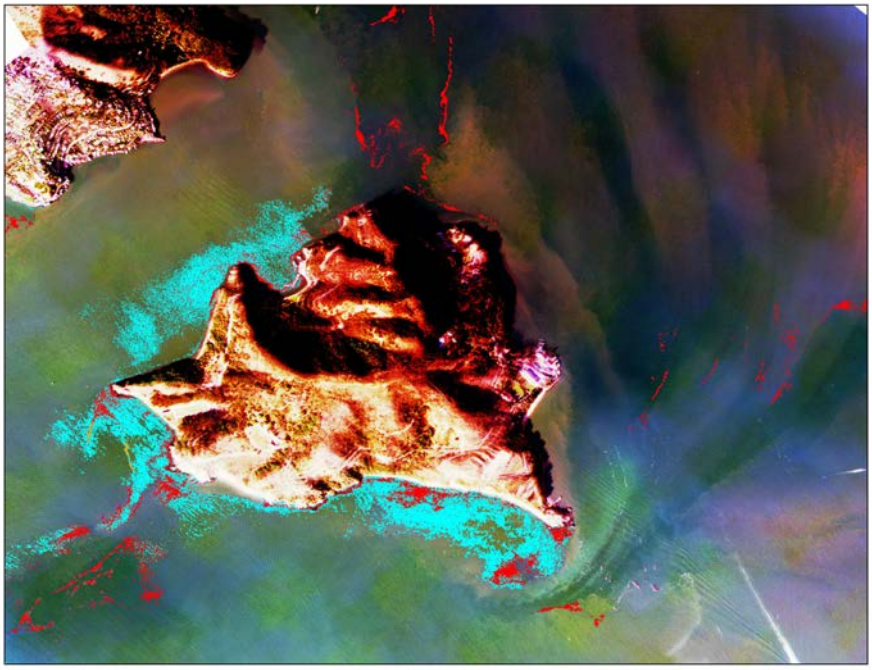

Principal Investigator: Dr. Jan Svejkovsky, Ocean Imaging Corp. 201 Lomas Santa Fe Dr., Suite 370, Solana Beach, CA 92075 (858) 792-8529, Fax: (858) 792-8761, jan@oceani.com

Co-Investigator: Judd Muskat, CDFG Office of Oil Spill Prevention and Response, 1700 "K" Street, Sacramento, CA 95814 (916) 324-3411, jmuskat@ospr.dfg.ca.gov

Acknowledgement

This project was funded by the U.S. Minerals Management Service. The authors wish to thank the U.S. Minerals Management Service, Engineering Branch for funding this study and Joseph Mullin for his guidance in the work. Thanks also go to the California Department of Fish and Game, Office of Oil Spill Prevention and Response for providing the plane and pilot for the remote sensing experiments over the Santa Barbara, CA oil seeps, to Mr. Merrill Jacobs and Mr. Rick Gill of Clean Seas LLC, Carpinteria, CA for providing the vessels and crew to assist in the technology demonstration exercise over the Santa Barbara, CA oil seeps in October, 2008, and to the staff of the Ohmsett Facility for their assistance in conducting daytime and nighttime tests at Ohmsett in the summer of 2008.

Disclaimer

This report has been reviewed by the U.S. Minerals Management Service staff for technical adequacy according to contractual specifications. The opinions, conclusions, and recommendations contained in the report are those of the author and do not necessarily reflect the views and policies of the U.S. Minerals Management Service. The mention of a trade name or any commercial product in the report does not constitute an endorsement or recommendation for use by the U.S. Minerals Management Service. Finally, this report does not contain any commercially sensitive, classified or proprietary data release restrictions and may be freely copied and widely distributed.

On the Cover: Multispectral data classified for oil distribution and thickness showing part of San Francisco Bay during the M/V *Cosco Busan* oil spill, imaged by Ocean Imaging on 11/9/07.

TABLE OF CONTENTS

EXECUTIVE SUMMARY

This project represents an expanded follow-on effort aimed to develop a hardware/software system that would enable near-real-time mapping of an at-sea oil spill and its thickness distributions. In November 2005, the MMS initiated a research project to develop an algorithm that would enable the measurement of oil slick thicknesses using multispectral aerial imagery and to evaluate the feasibility of developing a relatively economical, portable aerial oil spill mapping system that could be operationally deployed. Such a system would enable rapid oil spill mapping with greater quantitative and geographical accuracy than is presently possible using visual observations. The California Department of Fish and Game's Office of Oil Spill Prevention and Response (CDFG/OSPR) partnered with MMS on the project and provided technical expertise with the project's Geographic Information System (GIS) components as well as services in kind (plane and pilot). An oil thickness measurement algorithm was developed that utilized 4 customized wavelengths in the visible range from a multispectral aerial sensor. Using data obtained under small-scale laboratory conditions, larger-scale experiments at Ohmsett (the National Oil Spill Response Test Facility in Leonardo, New Jersey), and aerial and ship-based field sampling of slicks from natural oil seeps in California's Santa Barbara Channel, the oil thickness algorithm was developed and validated for light and medium weight crudes and several IFOs. Due to spectral reflectance properties of these oils the usable thickness range of the initial algorithm proved to be from sheens to approximately 0.15-0.2mm. Thicker oil films could still be positively identified and their distribution mapped but their true thickness could no longer be distinguished. Results from the initial project proved that the development and operational utilization of a portable multispectral imaging system for oil spill mapping is very feasible and could provide major improvements in oil spill response.

In October 2006, the MMS initiated a second research project to develop a portable, easy-to-operate, aerial sensor to detect and accurately map the thickness and distribution of an oil slick in coastal and offshore waters in near-real-time. CDFG/OSPR partnered with MMS again on this project and provided technical expertise and similar services in kind. One of the major accomplishments in this follow-on project was the expansion of the initial algorithm's effective thickness measurement range to several millimeters with the addition of a thermal infrared camera to the system. Algorithm refinement and validation were again done at Ohmsett and over the Santa Barbara seeps. The thermal imager also proved to allow the mapping of refined petroleum products such as diesel, jet fuel and lubricant oils that have no distinct color reflectance characteristics at thicknesses usually encountered in an at-sea or harbor spill. The thermal imaging also added nighttime mapping capabilities.

In synergy with a concurrently running project funded by CDFG/OSPR, the developed aerial mapping system was incorporated with a web-accessible GIS which provides response and command crews near-real-time access to the fully processed, auto-geolocated oil spill maps. The near-completed system was utilized experimentally by OSPR during the M/V *Cosco Busan* oil spill in San Francisco in November, 2007. The full system was successfully demonstrated to multiple agencies, California State representatives and the media in a field exercise in Santa Barbara, California in October, 2008. Following this demonstration, the system was successfully utilized in full operational mode during a platform spill in the Santa Barbara Channel in December, 2008. The developed oil mapping capabilities are available for use during future spills in California and elsewhere.

1. PROJECT BACKGROUND

1.1 Present-day Oil Spill Assessment Techniques

One of the most important initial steps in response to an oil spill at sea is the assessment of the extents of the oil slick and the quantity (i.e. thickness) distribution of oil within it. Since many types of hydrocarbons rapidly spread out to very thin layers when released at sea, accurate determination of which areas contain the most amount of oil is vital for efficiently guiding oil spill response efforts. Addages often mentioned by response crews such as "80% of the oil is contained in 20% of the slick" and "wasting time chasing sheens" illustrate the common, frustrating problem of misallocating time and resources due to insufficient knowledge of the oil thickness distribution within a spill.

The vast majority of oil quantity distribution assessments are presently done visually from helicopter or aircraft. Figure 1. shows thickness guidance parameters based on oil film appearance, which are commonly included in oil spill response training guides throughout the world. Such visual observations from aircraft (sometimes supplemented by drawings or digital photographs) suffer from three main complications. First, any verbal , graphic or oblique photographic documentation is usually based only on approximate geolocation information obtained through the aircraft's GPS. Even if it is later reformatted as input into a computerized Geographical Information System (GIS), the data can contain a great degree of positional error. Second, visual estimation of oil film thickness distribution is highly subjective, is affected by varying light and background color conditions and, if not done by specially trained and experienced personnel, tends to be inaccurate. Most often the observers' tendency is to overestimate the amount of oil present. Third, comprehensive visual assessments are impossible at night.

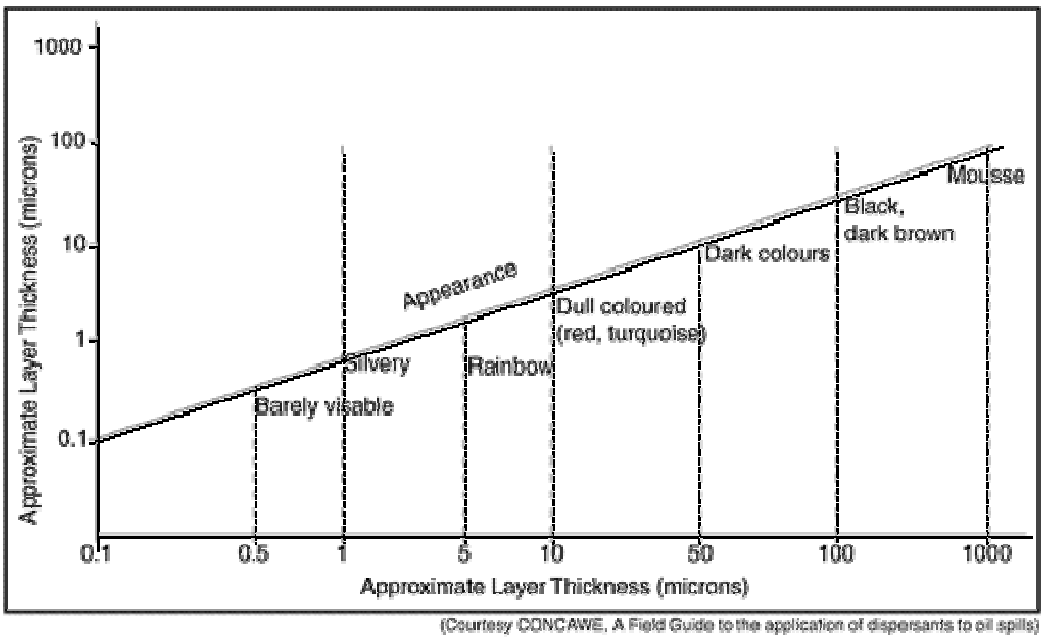

Figure 1. Oil-on-water appearance related to its thickness for guiding visual assessments. (From Gillot et al. 1988)

1.2 Project's Objectives and Approach

Our premise was to develop an aircraft or helicopter deployable system that would utilize the same universally tested and accepted spectral reflectance relationships between oil film thickness and its color appearance, but to eliminate the above-mentioned problems associated with visual observations by employing standardized multispectral camera systems for the imaging, and objective digital algorithms for the thickness estimation mapping. The addition of highly accurate geolocation devices to auto-georeference the imagery would also allow high location accuracy and the creation of a GIS-compatible, high resolution oil spill map product in near-real-time. An important consideration was to develop a system around relatively inexpensive, off-the-shelf hardware rather than a one-of-a-kind experimental or research-grade system that would have limited operational use.

An initial, OSPR-funded effort showed that crude oil at sea (e.g from natural seepage) can be reliably identified and separated from numerous artifacts and false targets with a multispectral digital aerial camera system imaging in the 400nm – 900nm range (Svejkovsky 2007). Based on this background work, MMS funded Ocean Imaging (OI) and OSPR to expand the research and develop methodologies to include oil thickness information in the generated maps. OI utilized its own multispectral system – the DMSC MkII, manufactured by SpecTerra Ltd. in Australia. A 2-step algorithm approach was developed: a neural network-based algorithm is first applied to the data to create a binary oil/no-oil mask; a fuzzy ratio-based algorithm is then used on the oil-contaminated pixel areas to bin them into several thickness classes based on ratio relationships of the different wavelength channels compared to channel ratios of non-oiled areas (i.e. existing water background reflectance) (Svejkovsky and Muskat 2006, Svejkovsky et al. 2008). The method was validated and found to be robust but, as is the case with visual observations, crude and IFO color signatures attain their "full, true color" at 0.15-0.2mm thickness and thicker films can no longer be accurately distinguished and classified with image bands in the UV-Visible-nearIR range. Previous work with thermal IR sensors done in Europe suggested the potential for IR imagers to have increased thickness detection capabilities for thicker oil films (Byfield 1998, Davies et al. 1999). On the other hand, sheens and thin oil films tend to not be distinguishable in IR imagery. Our approach in this follow-on project was therefore to combine the multispectral visible and IR systems and thus extend the measurable thickness range. This combined approach has not been sufficiently explored before and takes advantage of the overlap in discernible thickness ranges by the two sensor types for calibration purposes.

Our results from at-sea tests during the initial projects also showed that a system integrated solely with a differential GPS (DGPS) for geolocating the images will not yield acceptable positional accuracy under operational conditions. High geolocation accuracy in top-end aerial camera systems is traditionally achieved by using integrated Inertial Motion-detection Units (IMUs) that, in addition to instant position reading, also provide extremely precise roll, pitch and yaw information that can be used to recompute each image frame's true geographical coverage. IMUs with accuracies needed for precise aerial photogrametry tend to be relatively expensive ($85K-$200K), significantly raising the overall system's price. In the continuously dynamic ocean environment, positioning accuracies of one or two meters (or even a few meters) are not deemed critical for a large-scale oil map product – hence the initial consideration that an IMU may not be needed for the system. However, under a variety of

operational conditions the aircraft's roll, pitch and yaw cannot be adequately maintained at a constant and their variability causes 50 – 100+ meter positioning errors at 1500 –3,500 meter flight altitudes. This was deemed unacceptable for a useful, operational map product. In the follow-on project we therefore seeked to evaluate the potential to utilize lower-cost production IMUs ($8K - $35K), to establish if such instruments could provide the needed, yet economical autogeoreference solution.

With supplemental funding provided by OSPR we also strived to develop a system for efficient dissemination of the oil thickness map information that would enable various response units and agencies to access the information in near-real-time and use it to guide oil spill response strategies and resources.

2. PROJECT RESULTS

The project work objectives and schedule were divided into the following tasks:

Task 1 - IR Camera Integration and Testing
Task 2 - Oil Thickness Algorithm Refinement
Task 3 – IMU Unit addition and real-time mosaic testing.
Task 4 – OHMSETT Testing and Data Analysis
Task 5 – Full System Integration & Implementation of Real Time Analysis Delivery

These project phases are discussed sequentially below:

2.1 Task 1 - IR Camera Integration and Testing

The initial work for this task involved researching various off-the-shelf thermal camera options for suitability to map oil spills and their thickness distributions. In addition to technical capabilities, the cost of each unit was also considered, since the prime objective of this project was to develop an oil spill mapping system whose relatively low cost allows its purchase and use by numerous regional agencies. For this reason, cooled IR systems, while providing the best thermal sensitivity and largest pixel array options, were deemed too expensive ($100+K) for the project's application. IR cameras utilizing recently declassified uncooled microbolometer technology were chosen as the prime candidates for our objective. Upon evaluative demonstrations from several manufacturers, OI committed to purchasing a TCM640 camera from Germany's Jenoptik. Until late 2006, bolometer IR cameras were limited to a 380x280 pixel (or similar) detector size. In 2007 Jenoptik began offering camera versions with 640x480 pixel detectors, which for the purposes of aerial oil spill mapping vastly improves image spatial resolution and/or imaged swath width. Another consideration was the unit's capability to provide calibrated data (vs. an uncalibrated greyscale image). Calibration is not necessary for some applications – e.g. gun sights or search and rescue where only the identification of objects within the image, regardless of their true temperature, is needed. For linking an oil film's thermal emissivity to its thickness, however, true calibrated data are required to achieve repeatable results.

The camera was ordered in mid-June, 2007 and OI took delivery in October, 2007. It should be noted that the camera was purchased with OI internal funds not associated with MMS' funding of this project. In addition to the hardware purchase, OI reached a cooperative

agreement with Jenoptik to develop unique software which will allow the exportation of captured image frames from Jenoptik's proprietary format to a general GIS-compatible format for further processing and analysis, and will create an ancillary information file for each captured frame containing center-frame DGPS coordinates and time as well as other information needed to accurately georeference each image. This software was delivered simultaneously with the camera hardware and OI also internally wrote additional software for integration of the IR camera to OI's existing multispectral system.

The IR camera was successfully integrated with OI's DMSC multispectral imager in November, 2007. The two systems are mounted side-by side in the aircraft and can be triggered to acquire image data either separately or simultaneously. Figure 2. shows sample separate and merged imagery over a portion of the San Diego coastline.

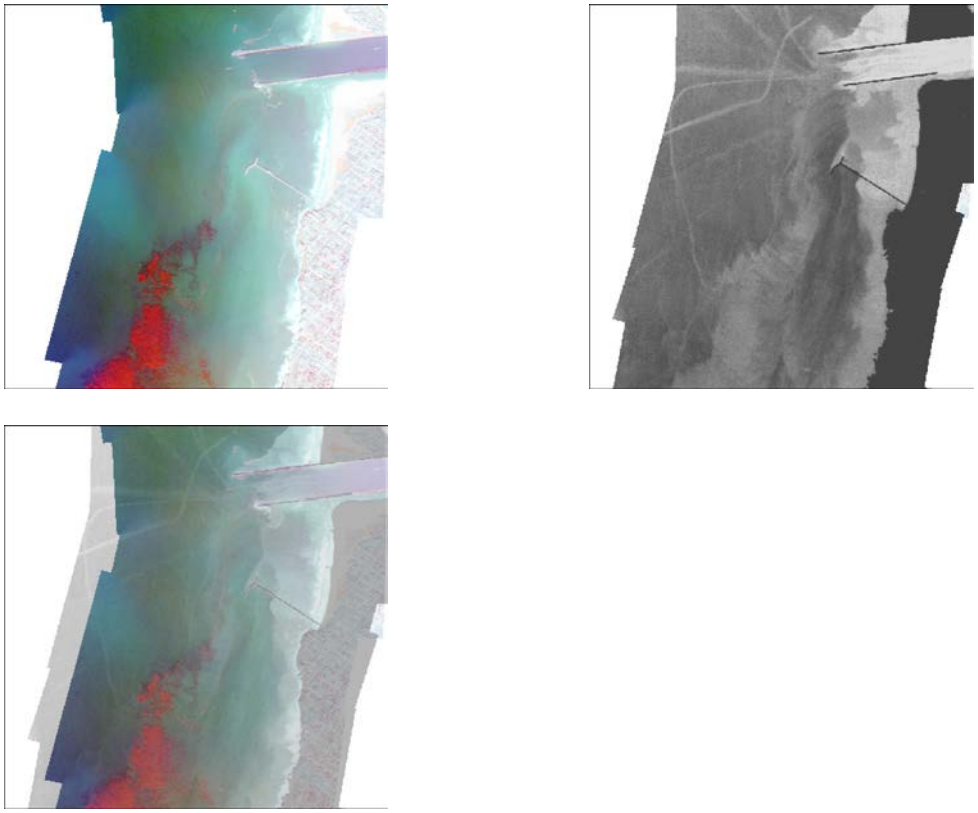

Figure 2. DMSC visible multispectral image of the Ocean Beach Pier/Mission Bay Entrance area (upper left), and same area imaged with the thermal system (upper right). The red features in the DMSC image are kelp seaweeds. The linear features in the thermal image are residual (cool) boat wakes. Also note the cooler (lighter) circulation patterns nearshore related to the Bay entrance jetties and the pier. A merged composite from the two systems is shown at lower left.

2.2 Task 2 - Oil Thickness Algorithm Refinement

This work, undertaken simultaneously with Task 1, involved the majority of labor expended on this project. Data obtained during the Phase 1 Oil Thickness Measurement Project during 2005-2006 were re-analyzed for optimal wavelength characteristics that

provide the maximum oil thickness discrimination capabilities utilizing the thickness classification algorithm developed in the earlier project. This re-analysis resulted in the change of one of the DMSC's channel wavelengths.

With the new 4-channel wavelength configuration, new experiments were conducted utilizing both a downward-viewing spectrometer and the actual DMSC aerial sensor. With the aid of San Diego-based commercial fishermen and the local harbormaster, a test area was constructed where small quantities of oil films of known thicknesses were contained over deep water with no or minimal bottom reflectance, thus approximating the influence of water color and scattering characteristics existing in a "real-world spill" situation. Numerous experiments were conducted on different days and under different atmospheric and sun-angle conditions using several samples of crude supplied to OI by MMS' Ohmsett facility during the initial project. Following each series of measurements all the contained oil was recovered and disposed of as per pertinent regulations at a nearby automobile service facility.

As can be seen from example results shown in Figure 3, band ratios (on which the developed thickness algorithm is based) between the chosen 500nm and 600nm bands are very sensitive to oil film thickness when compared to the clear-water background signal. Compared to the results of algorithm development during the initial project we achieved two significant improvements: 1) the 577nm band (which was not used in the initial algorithm) provides the greatest thickness distinction range of ratios and 2) when used in conjunction with the 551nm band the clear-water background reflectance differences between the two wavelengths provide information effectively used by our algorithm to adjust the thickness model for different background water reflectance characteristics. As was expected based on results from the initial project, the absolute thickness detection limit for the algorithm using only the chosen four channels in the visible part of the spectrum is approximately 0.2mm. (Thicker oil is detected but reflectance spectra characteristics do not change sufficiently to determine its absolute thickness.) The thickness algorithm software was modified and the final thickness decision tree based on the new results was incorporated.

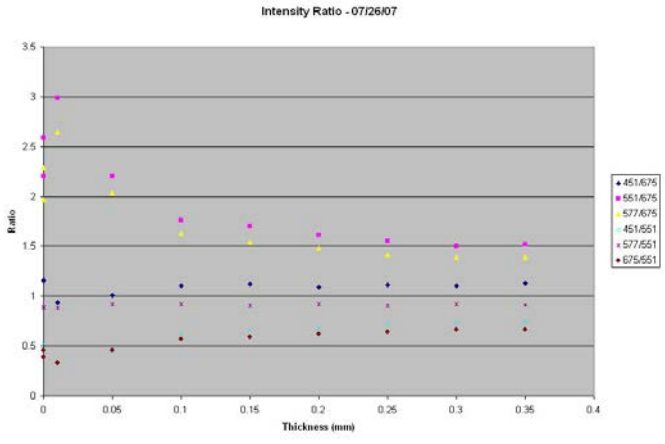

Figure 3. DMSC band ratios of oil film reflectance over deep water using Alaska North Slope crude.

Additional experiments were conducted in an enclosure in San Diego Bay that provided further data to refine the "signature files" used in the Fuzzy-ratio-based oil thickness determination algorithm developed earlier. The results proved highly repeatable under different sun angle and atmospheric conditions and thus provided a high level of confidence for the algorithm. Figure 4 shows the results of 9 such experiments, exemplifying the two most useful wavelength ratios for oil thickness assessment.

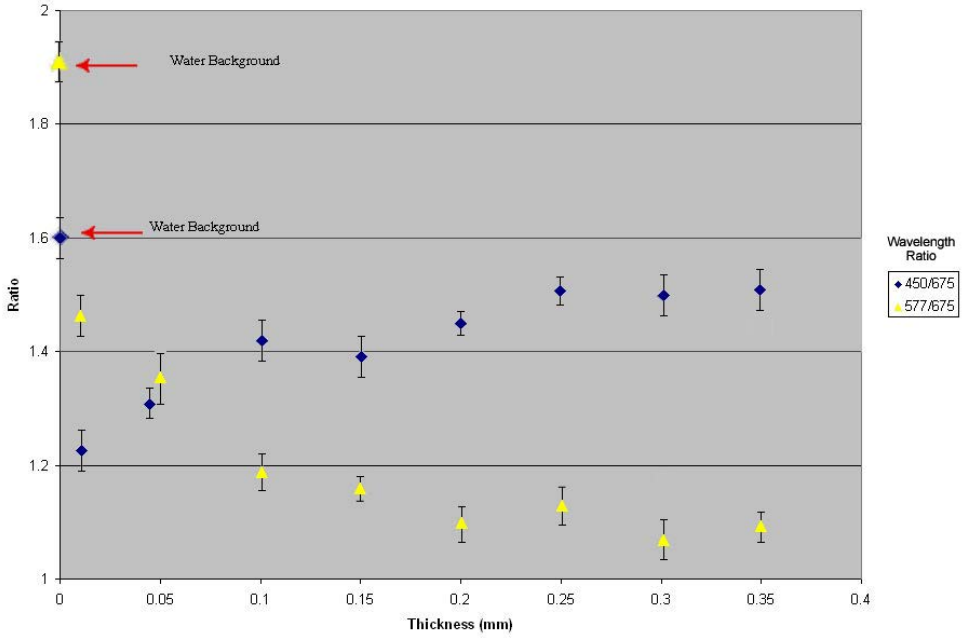

Figure 4. Two different wavelength ratios obtained at various thicknesses of ANS crude oil films over a deep water background.

Further work was done to automate the oil thickness mapping process, although the initial neural network algorithm that is used to identify and mask non-oiled water surface and potential artifacts requires a user-assisted "training" procedure that can be completed in 5-10 minutes. Experiments during previous and follow-on (see below) missions over the Santa Barbara Channel oil seeps proved that this operator intervention is necessary to eliminate or minimize artifacts (e.g. sun glint and kelp).

Experiments were conducted again in the Santa Barbara Channel on 12-13 December, 2007. A CDFG aircraft was used to guide a ship-based field sampling crew (on a commercially chartered 35' vessel) to the best oil target areas and to obtain simultaneous multispectral visible and thermal IR imagery. The field crew sampled oil thicknesses in each target area using techniques described in previous reports.

The objectives of the Santa Barbara work were to 1) obtain additional "in the field" validation data for the developed thickness algorithm and 2) to obtain field data with both the visible and IR systems integrated. These were then used for further research on how the addition of an IR channel can expand the algorithm's thickness measurement range. Figure 5 shows a surface oil feature classified for thickness using the multispectral algorithm. The thermal data (also shown) were classified for thickness based on field measurements. The extended range of thicknesses distinguishable in the IR image is readily shown. Just as important, however, is the observation that the two image types overlap in their oil sensing range. This allows the possibility of "calibrating" the IR signal with information computed from the multispectral data. To our knowledge, this has not been attempted before by other researchers, who used one of the two systems independently. (Thickness determination from IR imagery independently is subject to environmental variables and is thus prone to variability without additional field information.)

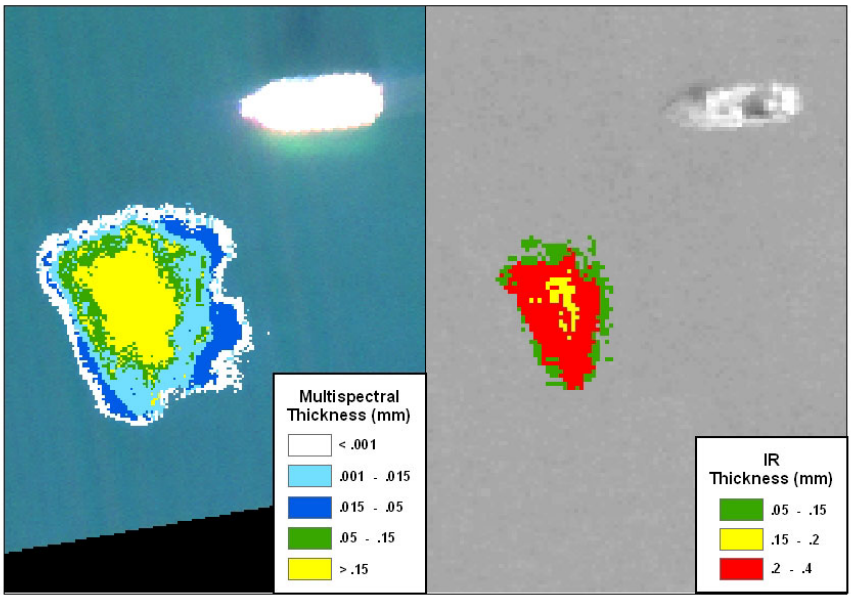

Figure 5. Oil slick feature in the Santa Barbara Channel imaged simultaneously with the multispectral visible (left) and thermal IR (right) sensors, and classified for oil thickness (see text).

The oil algorithm development and testing, and other work related to this project were presented in a plenary session at the International Oil Spill Conference in Savannah, Georgia 4-8 May, 2008. A peer-reviewed paper describing this project's research and results was published in the Conference's Proceedings (Svejkovsky et al. 2008)

2.3 Task 3 – IMU Unit addition and real-time mosaic testing.

An operational oil spill mapping system should have the capability to not only accurately map the oil thicknesses but also generate a geographically accurate map of the spill's location. Logged DGPS information for each captured image frame theoretically provides an accurate position for the center of each frame. However, it does not provide information on the roll, pitch and yaw of the aircraft at the time of each frame capture. The lacking of these parameters introduces positional errors in the autogeoreferencing/mosaicking software. At aircraft altitudes of 10,000' we found these errors to cause individual frames to be up to 100 meters, thus creating an uneven image mosaic.

When flying over land, visible features present in the overlap area of succeeding image frames can be used to correct much of the positional error by fitting the individual frames to a base layer image or map of known accuracy (this can be done either manually or automatically with commercially available pattern recognition-based mosaicking software). When imaging over open ocean, however, such tie-point features are usually lacking and the roll/pitch/yaw error is thus not easily determined and corrected.

Roll, pitch and yaw information is provided by Inertial Motion detection Units (IMUs). IMUs are used in a variety of navigation equipment (e.g. aircraft autopilots) as well as for testing purposes and aerial photography. Their price range is from approximately $4000 to $150,000+. The upper price range units are commonly integrated with state-of-the-art aerial imagers costing $500,000 to $1,000,000. One of the prime objectives of this project is to develop an oil mapping hardware/software system that would be accurate and efficient, yet reasonably economical and hence affordable to various agencies and other oil spill responders. We thus evaluated the suitability of various lower-cost IMUs for the purposes of mapping oil spills with sufficient accuracy.

Evaluation of accuracy specifications of several sub-$10K IMUs revealed that they will not provide either sufficient measurement accuracy or sufficiently high logging rate to significantly reduce the inherent positioning errors. Units made by Applanix Corp. – the most commonly used for high-end aerial measurement and imaging equipment – provide excellent overall performance but cost from $80,000 to $200,000. This was deemed excessive in view of the targeted overall system cost (@ $100,000).

During spring 2008 our research team located a British IMU manufacturer – Oxford Technical Solutions - whose line of mid-priced IMUs includes units with theoretically acceptable performance specifications. The company's US representative kindly provided Ocean Imaging with a demo unit for actual real-world testing. An RT2500 unit (costing approximately $25,000) was tested in overflights over San Diego in the CDFG Partenavia aircraft in May, 2008. Figure 6 shows a typical result achieved when this unit was integrated with the thermal IR system (similar results were achieved with the multispectral DMSC). At 10,000' altitude, RMS positioning errors were reduced from 100+ meters to 5-8 meters. In light of the fact that oil on water constantly moves due to

wave, wind and current action, and the image data processing and transmission can be expected to take 10-20 minutes, we deem a positional error of less than 10 meters at 10,000' flight altitude quite acceptable. Therefore, we recommend the Oxford Technical Solutions RT2500 IMU unit for the targeted oil mapping aerial system. Following these tests OI purchased (from non-MMS funds) an upgraded unit (reducing RMS spatial error to <5m), RT3000 for $30,000 which was used in all subsequent work related to this project..

Figure 6. Auto-georeferenced imagery of San Diego coastline using only DGPS coordinate information (top) and using DGPS/IMU information (bottom).

2.4 Task 4 – OHMSETT Testing and Data Analysis

The Ocean Imaging (OI) research team visited MMS' Ohmsett Facility during 16 – 20 June, 2008. The prime objectives of the planned tests were:

1. Determine the relationship between thermal IR emission and oil thickness during both day and night (i.e. no solar input) conditions.
2. Investigate diurnal heating effects on oil film IR emissions.
3. Validate the multispectral oil thickness determination algorithm developed previously.

A new objective was added shortly before the Ohmsett trip at the request of the US Navy, who became aware of the project in the spring of 2008. The Navy is interested in developing an oil spill sensing system based on an Unmanned Aerial Vehicle (UAV) for use in recognizance around their ships and harbor facilities for petroleum leaks and spills. For obvious reasons, the Navy's interest is in detecting refined petroleum products such as diesel, jet fuel and lubricating oils – not crudes. This project's original focus was on crudes and IFOs, so refined products were added to the testing schedule during this time period. The final objective of work at Ohmsett was thus:

4. Determine best imaging wavelength configuration for on-water detection of diesel and other refined oil products. Full results of tehse Ohmsett tests, additional laboratory and aerial tests and hardware recommendations for this application are contained in a Final Report prepared for Navy-SPAWAR (Svejkovsky, 2008).

Because the Ohmsett tank is relatively shallow and the bottom and sides are painted white, we used a large blue-green canvas tarp, stretched out and weighted down on the bottom to reduce bottom reflection and mimic deep ocean water color reflectance. Canvas proved to be an excellent choice, since it remained stretched flat on the bottom and did not reflect sunglint as did a plastic tarp used on our previous Ohmsett tests.

The same oil-container set-up used during our 2006 Ohmsett work was used during these experiments: 4' x 4' floating squares made of grey PVC pipe were affixed in series in the tank and known volumes of oil were then poured into each square. The oil was further manually dispersed with a whisk-broom on a long pole. The objective was to disperse the oil in each square into a homogenous film whose thickness is computed from the total volume poured. The procedure worked during some experiments and with thick (>1mm) films. A fairly stiff breeze caused the spread-out oil to quickly pool toward one side of the squares in some instances, causing each square to contain areas of several different thicknesses. Since the total oil quantity was known, however, the experiments still provided useful data for testing the developed algorithm: the various thickness areas within each square were classified with the algorithm, the total oil volume was computed from the thickness distributions and the results were compared to the actual volume poured in.

Each experiment used all of the squares by imaging them as the tank bridge slowly moved (0.5 knot) over them.

Results Summary: Determine the relationship between thermal IR emission and oil thickness during both day and night (i.e. no solar input) conditions: Numerous experiments were conducted during which various oil types and thicknesses were imaged simultaneously with the visible multispectral DMSC and thermal IR sensors. Figure 7. shows a typical data set from a daytime (clear sky) experiment. There is a clear correspondence between the multispectral color and thermal IR oil signals: increasingly thicker oil films appear darker in the multispectral data and warmer in the IR data. This was expected, since the darker, thicker oil traps solar heat input during the day and thus increases in temperature relative to the surrounding water. The data also show that films thinner than approximately 0.05mm appear (under the existing winds and air/water temperatures) cooler than the surrounding water. This is in agreement with published finding of other researchers. The phenomenon is due to the lower emissivity of petroleum products compared to water. Since the thin films are not able to retain significant solar heat input, they have a cooler apparent temperature.

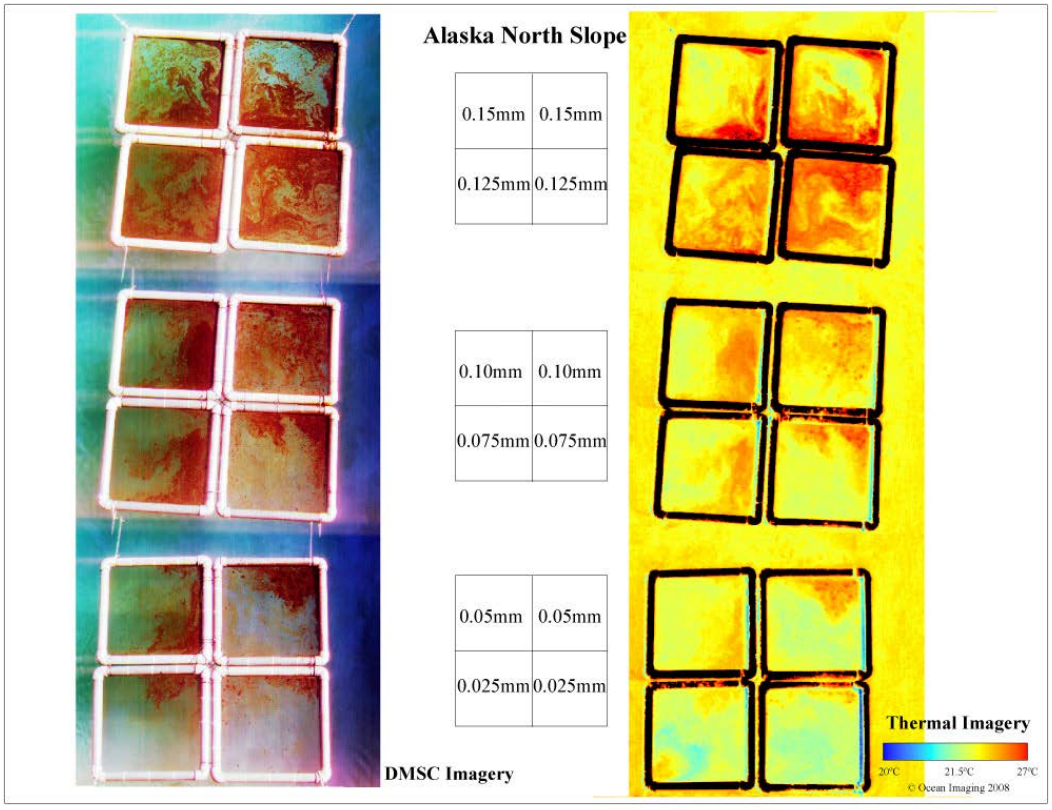

Figure 7. Alaska North Slope crude as imaged under sunny skies with visible multispectral (left) and thermal IR (right) systems.

The numerous image sets thus obtained provided both, data to test and validate the algorithm formerly developed for the multispectral color data (see below), and investigate the relationships between the color and thermal oil signals.

The primary reason for our adding a thermal IR camera to the thickness detection system was to potentially extend the measurable thickness range. Previous work repeatedly showed that the maximum thickness of crude and IFO oils distinguishable with multispectral imagery in the UV-Visible-nearIR range was approximately 0.1-0.2mm. Oil thicker than that can still be readily spatially mapped, but its thickness can no longer be determined (i.e. its spectral reflectance no longer changes). Since it is especially the thicker oil films that trap solar heating, a thermal IR image could potentially differentiate thicker films based on their thermal emission (rather than color reflectance) characteristics. Some limited tests of this concept were done during earlier work in this project over the Santa Barbara oil seeps and proved promising. Additional, controlled testing was done at Ohmsett. Figure 8 shows sample results: Figure 8A shows an ANS crude oil film sequence as imaged and classified from the DMSC multispectral data. As expected, oil thickness differentiation was possible up to approximately 0.15mm. Thicknesses in squares containing greater quantities of oil were lumped into the maximum thickness class. Figure 8B shows thickness classifications using simultaneously-collected thermal IR imagery. While the IR data show relatively poor thickness differentiation capability over thin films, they provide enhanced thickness differentiation over thicker films, particularly where the oil thicknesses were greater than approximately 0.2mm. Note, for example, that there was almost a 10ºC apparent temperature difference between films in the 0.5mm and 1.5mm range.

The (daytime) thermal response to thickness is even better illustrated in Figure 9, which combines data from several experiments. The graph shows that while thickness separation based on thermal signature is statistically poor below approximately 0.2mm, separation ability increases dramatically with increasingly thicker films. We continue to analyze the Ohmsett experiment results and are utilizing them to incorporate the IR channel into the thickness measurement algorithm. Since variations in wind, humidity, solar input and water/air temperatures will change the actual water/oil thermal contrast characteristics from one spill to another, we are concentrating on an adaptive approach in which we utilize thickness-related signals in the overlap region between the multispectral and IR instruments to “calibrate” the IR signal for thickness within each obtained image set.

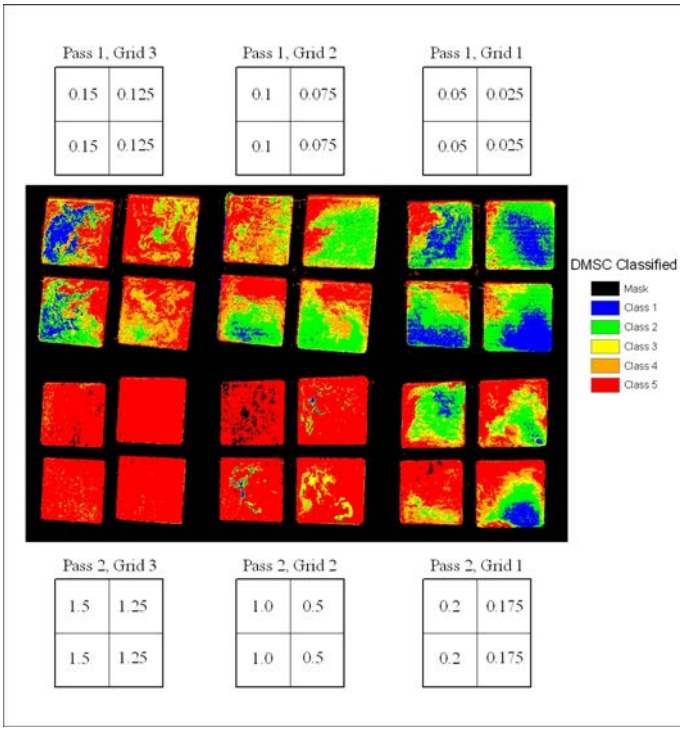

A.

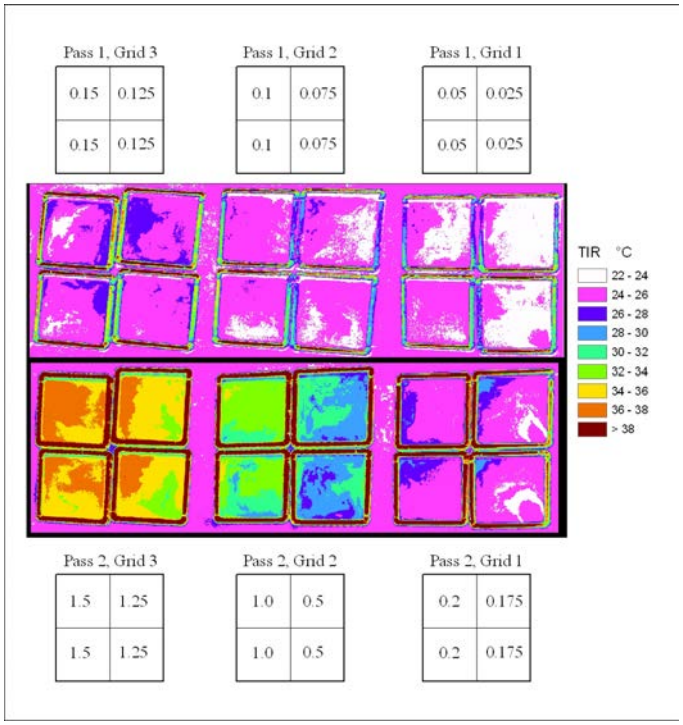

B.

Figure 8. Multispectral color image-based oil thickness classifications (top) and IR image-based classifications (bottom). Note the IR system distinguishes between the largest oil thicknesses which the multispectral system cannot differentiate.

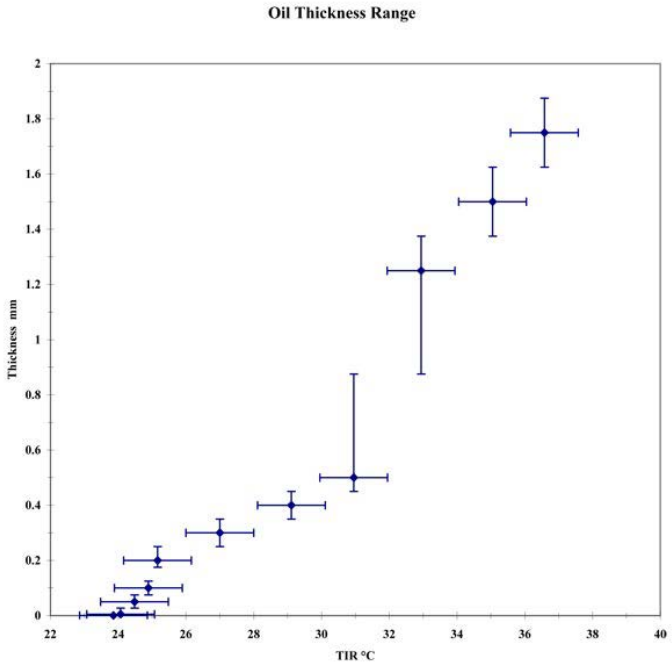

Figure 9. Oil film thicknesses found within shown temperature ranges as measured during daytime in the Ohmsett tank.

Results Summary - Investigate diurnal heating effects on oil film IR emissions: The general relationship between oil thickness and thermal camera signal during the daytime has already been mentioned and shown in Figure 1. To investigate the oil's thermal image response during nighttime (i.e. under no solar input), on 6/17/08 we continued the imaging experiments at Ohmsett past sunset. Figure 10 shows imagery of ANS and IFO-180 oils at 7pm (at a very low sun angle before sunset when the Ohmsett tank was no longer directly illuminated), and at 10pm. The data show that by 7pm the thickest oil films (which were 10+ºC warmer than the surrounding water at higher sun angles (see Figure 8B)) have lost the retained heat and are actually beginning to exhibit a cooler-than-water apparent temperature. Likewise, the thinner films tested, down to 0.05mm appear cooler than water. This contrast only becomes accentuated by 10pm. It should be noted that while the water temperature remained stable at 79.4 – 79.7F, the air temperature dropped from 72.4F at 7:45pm to 66.8 at 10:15pm. It must also be noted that at the 0.02 and 0.05mm thicknesses the IFO-180 was not spread adequately and most of the area within those squares was relatively oil-free, accounting for the apparently low thermal contrast between those squares and the surrounding water.

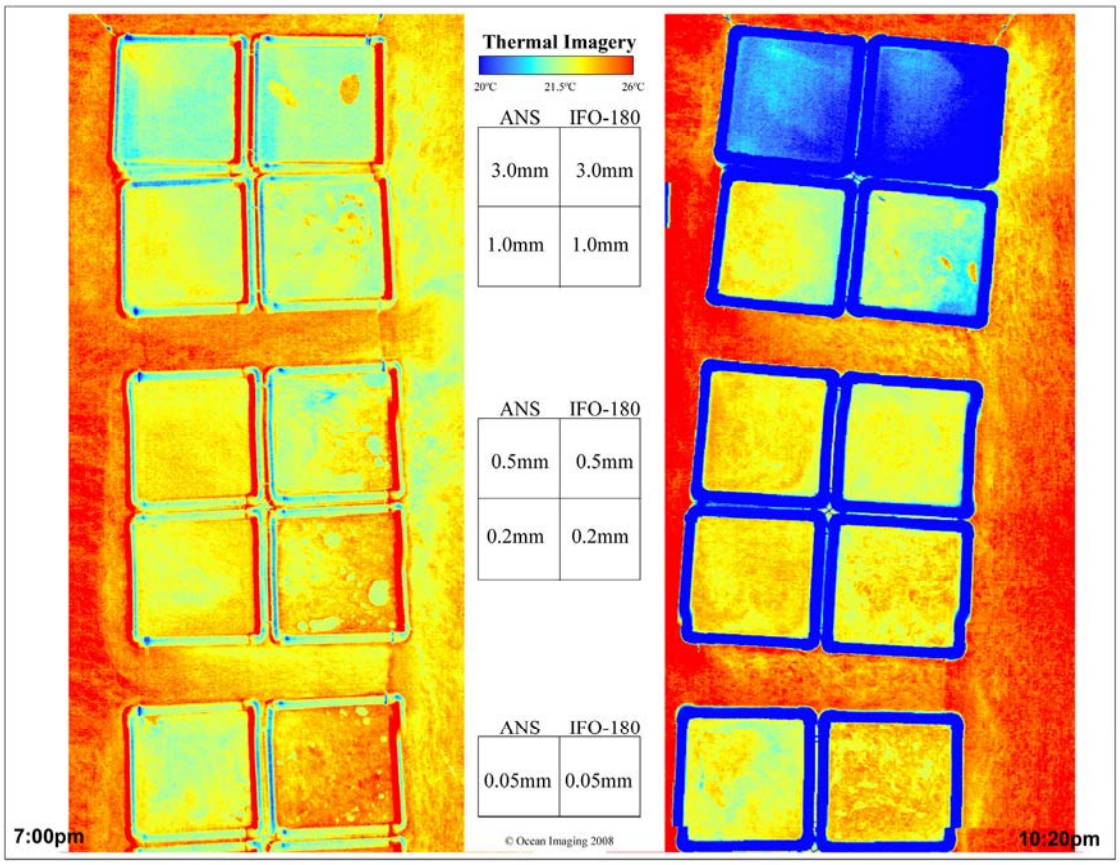

Figure 10. Thermal signatures of ANS and IFO-180 oil samples at different thicknesses at 7:00pm (very low sun angle before sunset) and at 10:20pm (nighttime).

Our Ohmsett nighttime results indicate that the addition of a calibrated IR camera to an oil spill mapping system can result in the added ability to map the spill at night with some thickness determination capability. Further nighttime tests were done recently using ANS as well as refined oil products at OI's San Diego facility using a backyard children's pool. One such data set is shown in Figure 11. The San Diego data support conclusions made from the Ohmsett tests.

One other finding should be noted in this progress report: It is generally recognized in published literature that IR imaging of oil fails to detect thin oil films. The most commonly cited lower thickness limit is 50um, however, most of those studies were done with IR instruments in the 1970s and 1980s and, to our knowledge, during daytime. Our new results from both Ohmsett and San Diego indicate that the lower thickness detection limit is significantly thinner during nighttime, closer to 10um for the oils studied.

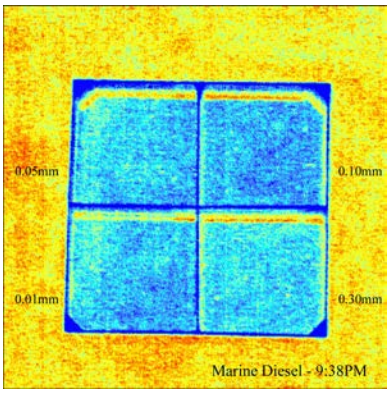

Figure 11. Marine diesel of different thicknesses imaged with the IR system during nighttime in a pool. Blue colors indicate cool apparent temperatures, surrounding water is warmer.

Results Summary- Validate the multispectral oil thickness determination algorithm developed previously. Results indicate that the developed algorithm could be successfully applied to the Ohmsett conditions (including the artificial "deep water" simulated by a colored tarp on the bottom) without major modification. The addition of the IR sensor allowed increasing the overall thickness measurement range as discussed earlier. Figure 12 shows our Ohmsett results: the imagery was classified for thickness classes (due to the wind effects most sample squares contained more than one thickness class) and from computation of each class' area the total oil volume in each square was determined. The results were compared to the actual oil volume poured into each square.

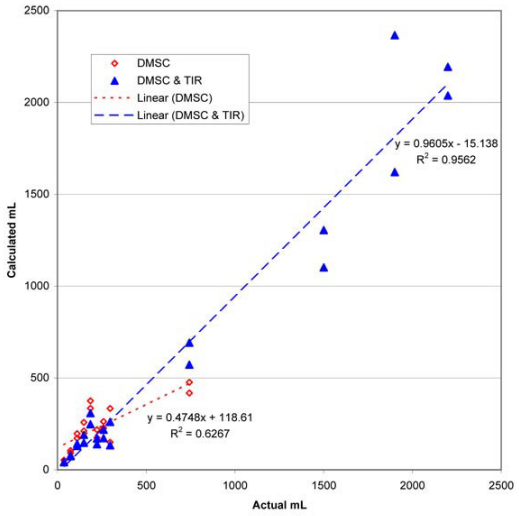

Figure 12. Oil volume in different squares in the Ohmsett tank computed from the image classifications vs. actual volume poured in each square.

Results Summary- Determine best imaging wavelength configuration for on-water detection of diesel and other refined oil products: Initial spectrometer and imaging tests were done at the Ohmsett Facility in New Jersey and at the pool site in San Diego. At Ohmsett, several thicknesses of marine diesel (containing red dye), JP-5 jet fuel and Hydrocal lubricant were imaged with Ocean Imaging's (OI's) 4-channel UV-Visible-nearIR, and thermal IR sensors. Continuous spectra of each sample were also recorded with an Ocean Optics portable spectrometer. In San Diego, several thicknesses of marine (containing red dye) and automotive (no dye) diesels were imaged with OI's 4-channel sensor and spectrometer. All image data were calibrated using reference radiance target data obtained during the imaging, and processed using ERDAS and ArcGIS image processing software.

Our measurements show that over the entire film thickness range that can be expected in a real-world spill situation, refined products have much less distinct color reflectance than crudes. Although jet fuel has a yellow tint in large quantities, undyed diesel appears blue-green and dyed diesel reddish, at expected on-water thicknesses of less than 1-2mm (due to their low viscosity these products will spread to much thinner films unless physically constrained), the subtle color tints do not significantly attenuate the underlying water color background. Crudes which tend to have a strong brown tint at film thicknesses between 0.01 and 0.2mm (thicker films appear near-black) alter the underlying water spectrum significantly in the visible wavelength range. Hydrocal also tends to have a noticeable brown tint, hence would be expected to possibly alter the background irradiance at thicker concentrations.

In both, the Ohmsett and San Diego tests, the tested refined products exhibited increased irradiance relative to the water background between approximately 430 and 550nm. We believe this is due to fluorescence from excitation by sunlight (fluorescence tails of most petroleum products reach into the 550-600nm range). Diesel spectra from San Diego also show strong increases in irradiance relative to water background in the UV region, approximately 350-400nm and likely down to 300nm (the spectrometer used significantly loses sensitivity below 350nm). Surprisingly, samples tested in the Ohmsett tank showed only very slight irradiance increases relative to the water background in the UV region. In addition, the irradiance signal of both the samples and "clear" water was much higher in the UV than at the longer wavelength regions. This is inconsistent with published water irradiance spectra. Since water strongly absorbs UV light, the ocean surface generally appears "black" in the UV region (for this reason, the inclusion of a UV channel in future ocean color sensing satellite instruments has been suggested for use in more efficient atmospheric correction algorithms). One explanation of the Ohmsett spectra results is that the Ohmsett tank water contained sufficient residual (both surface and dissolved) hydrocarbons to make the background signal in the UV region uncharacteristic – i.e. the tank water significantly fluoresces even without the addition of a hydrocarbon sample. This is possible because the Ohmsett water is reused for over a year by being recirculated through physical (diatomaceous earth and carbon) filter systems. Such filtration cleans particulates and undissolved oils is not effective against dissolved hydrocarobons. Additionally, small amounts of residual surface oil films were occasionally observed in the tank. We will conduct additional tests in San Diego to better

answer the Ohmsett observations. The Ohmsett staff also took samples of the tank water during OI's experiments and we will try to obtain chemical analyses of the samples.

Both Ohmsett and San Diego tests showed that irradiance differences between refined oil films and background water in the red and near-IR region are very small and thus unlikely to be useful for operational detection purposes. OI did not have an IR radiometer to obtain spectra in the IR region.

Imaging tests were done at Ohmsett by releasing a known amount of petroleum into floating containment squares and spreading the petroleum through the each square to achieve a film of known thickness. Thicknesses tested for marine diesel and JP-5 were 0.007mm, 0.05mm, 0.1mm and 0.4mm. Thicknesses tested for hydrocal were 0.014mm, 0.1mm 0.2mm and 0.4mm. The imager's 4 channels were loaded with 400nm, 451nm, 551nm and 675nm filters (10nm bandwidth). In concurrence with the spectrometer measurements, imaging diesel and jet fuel at the 400nm (long wave UV)wavelength showed the petroleum films to have slightly higher reflectance than background water. Accounting for variability in background and bottom reflectance within each square, no significant difference between water background and either of the fuels was detected at 451 and 551nm for any of the tested thicknesses. The more viscous hydrocal was more difficult to spread throughout the test squares and wind over the tank tended to herd it toward one side of each test square, causing an accumulation thicker than the original intended film thickness while the rest of each square area had only a thin film covering. At the 400, 451 and 551nm wavelengths, the thin film areas showed slightly lower reflectance than water and the thick film features exhibited significantly lower reflectance.

Also in concurrence with the spectrometer measurements, no significant difference was imaged at 675nm for any of the refined products, except for the thick (>0.1mm) accumulations of hydrocal which were more reflective than water.

All tested refined products at all thicknesses were readily detectable with the thermal IR imaging system. The emissivity of petroleum products is lower than that of water, hence a petroleum film on water should have a lower apparent temperature, even if in thermal balance with the underlying water. This proved to be the case in the imaging tests, with water-to-oil thermal contrasts of up to several degrees Centigrade. Even films thinner than those in the test squares (i.e. 0.0007mm) created by slight petroleum leakage around the squares were detectable due to a @1ºC contrast. It should be noted that at the time of these experiments the water temperature was 26.2ºC and the air temperature was 20.7ºC with clear skies and approximately 3-5knt winds. The oil vs. water thermal contrasts can be expected to change somewhat under different water/air/wind conditions.

The thick accumulations of hydrocal showed significantly higher-than-water temperatures. This was likely due to an actual thermal increase caused by trapping of solar heating by the thick, relatively dark oil film. Our observations are consistent with other published thermal imaging observations of crudes-on-water.

Based on the tests conducted to-date, a thermal camera system holds the most promise for detecting refined products on water under operational conditions – primarily because it provides the greatest water vs. petroleum contrast and would therefore offer the easiest image interpretation. The inclusion of an IR imagery on the UAV would also provide nighttime surveylance capability. We intend to conduct further tests to determine the utility of an IR system under different water and air temperature conditions, and also determine the minimal oil film thicknesses for refined products that can be reliably detected with an IR system.

Our tests also indicate that although there usually is a spectral irradiance difference between water background and refined petroleum films in the visible and near-IR part of the spectrum, it is likely not sufficient for routine oil detection under operational conditions. This also suggests that combinations of wavelengths in those ranges (i.e. multispectral ratios, etc.) will not provide sufficient detection capability for refined products.

Our San Diego tests and, to some extent, Ohmsett tests suggest that a UV imager may also be useful for refined oil product detection during daylight. Because of the possible contamination effects at the Ohmsett tank discussed above, we intend to conduct more experiments in San Diego targeting the imaging of various refined products with at UV wavelengths. Since the UV band detects signals even from very thin sheens that generally are not visible in IR imagery, a combined UV/IR UAV payload may allow better detection than a single instrument as well as differentiation capability between sheens and thicker petroleum concentrations. Such a combination is operationally used for aerial crude oil detection in Europe but, to our knowledge, has not been tested on refined products.

2.5 Task 5 – Full System Integration & Implementation of Real Time Analysis Delivery

The developed oil mapping system has been fully integrated. It consists of: a) DMSC multispectral imager; b) Thermal IR imager; c) IMU/DGPS; d) Sprint wireless data network modem; e) directional antenna for the wireless network. The system was operationally tested on 6/11/08 as part of a Chevron-initiated, multi-agency oil spill drill off San Diego. The system was mounted in California Dept. of Fish & Game's aircraft and flown over the drill vessel which dispersed fluoroscene dye to simulate an oil slick. The vessel and "slick" were imaged simultaneously with the DMSC and IR systems and the digital image data were then immediately sent to OI's server via the wireless data network from approximately 5 miles offshore. The data were then processed to "map" the oil slick an its "thickness" (simulated by dye intensity) distribution and posted on the multi-agency distribution GIS server developed by OI for CDFG's OSPR in an independent project. Total time between initial image acquisition and the final posting was 17 minutes. Figure 13 shows the original imagery as transmitted and the final classification posted on the GIS server..

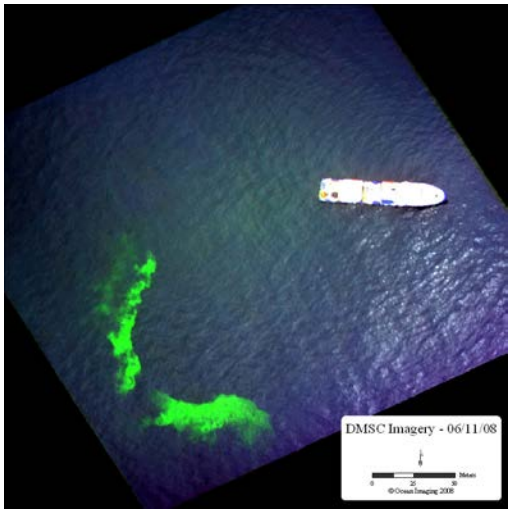

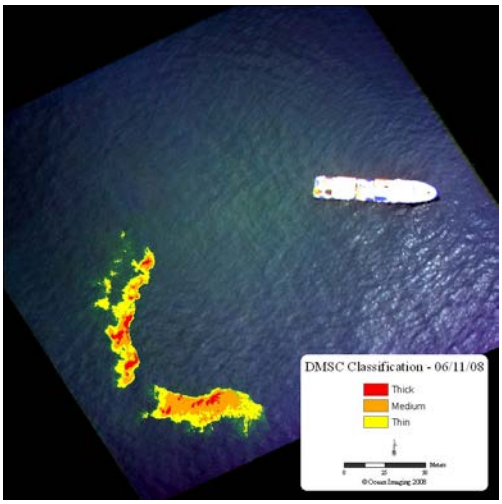

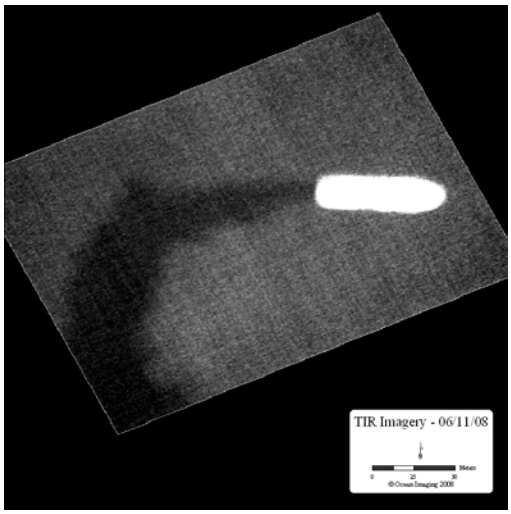

Figure 13. Multispectral (upper left) and thermal IR (lower left) imagery of the spill drill vessel dispersing dye simulating and oil spill. The images were sent to OI for processing directly form the aircraft. A GIS-compatible "oil" spill map (above right) was posted on a web-accessible server 17 minutes later for multi-agency access.

MMS and OSPR collaborated on staging a technology demonstration exercise in the Santa Barbara Channel on 11/13/08. The objective was to provide a wide audience with a hads-on opportunity to see the developed oil mapping system in action. A chartered vessel was used to bring the participants to natural oil seep areas in the Channel, where they were briefed on the nature and science of the seeps by UCSB researchers, and were shown a demonstration of oil boom and recovery equipment by Clean Seas who provided a vessel and equipment for the exercise. The participants then observed the CDFG aircraft conduct imaging flyovers over the oil features. Communication between the aircraft imaging crew and the observer vessel was conducted by radio.

The imaged data were processed in-flight and posted on the web-based GIS server. Upon the observer vessel's return into Santa Barbara Harbor, an on-line demonstration and discussion of the imaging results was provided to the participants. The demonstration was well attended, with representatives from MMS, OSPR, Clean Seas, the U.S. Coast Guard, state and local government, and the news media. A report and interview on the project was broadcast on National Public Radio and several newspaper articles were published.

3. SYSTEM APPLICATION IN REAL OIL SPILL EVENTS.

3.1 The M/V *Cosco Busan* spill in San Francisco Bay

At mid-day on 7 November, 2007 the cargo ship M/V *Cosco Busan* struck the Oakland Bridge in San Francisco Bay and spilled 58,000 gallons of IFO-380 bunker fuel into the Bay. Our project partner, Judd Muskat from CDFG/OSPR, arranged for OI to have access to the CDFG aircraft on the 9th and OI thus imaged a large portion of the spill area approximately 48 hours after the initial spill.

The imaging was done with the 4-channel DMSC at wavelength combinations determined by the previous work. Unfortunately, power could not be adequately installed for the IR system within the plane to also obtain simultaneous thermal data. (OI and the pilot/plane mobilized within 3 hours of the OSPR notification.) The data were subsequently processed using algorithms developed for this project.

Several factors proved to be different in this spill than would be expected during a "typical" oil spill at sea. First, the extremely strong tidal currents within the Bay caused the initial spill to be rapidly advected away from the spill site and the initial slick to be torn into small sections that widely separated from each other. By the time of our imaging overflight no actual oil slick existed. Rather, the thicker oil was distributed in narrow (2-4m wide) strands that were mostly aligned with current shear zones existing at that particular time. Some sheen-dominated areas also existed but were likewise widely distributed. Second, due to air traffic from multiple airports in the region, our imaging altitude was limited to either below 2000 or above 10,000 feet. Since the imaging swath would be extremely narrow at 2000', we did our scanning at 10,500', resulting in approximately 1.7m spatial resolution data – significantly coarser than we would have prefered. Third, the Bay's extreme variation in suspended sediment patterns within the oiled area resulted in highly variable background reflectance characteristics.

The narrowness of the oil features relative to the image resolution (i.e. each thick oil strand was only 2-3 pixels wide) proved to be the most detrimental factor for the application of the oil detection and thickness classification algorithm – primarily because very few “pure” oil pixels, not partially contaminated with neighboring water signal, were available to train the neural network. The algorithm was successfully applied, however, and the oil areas were identified and classified into two thickness classes, as exemplified in Figure 14. Since OI was not able to also conduct simultaneous field

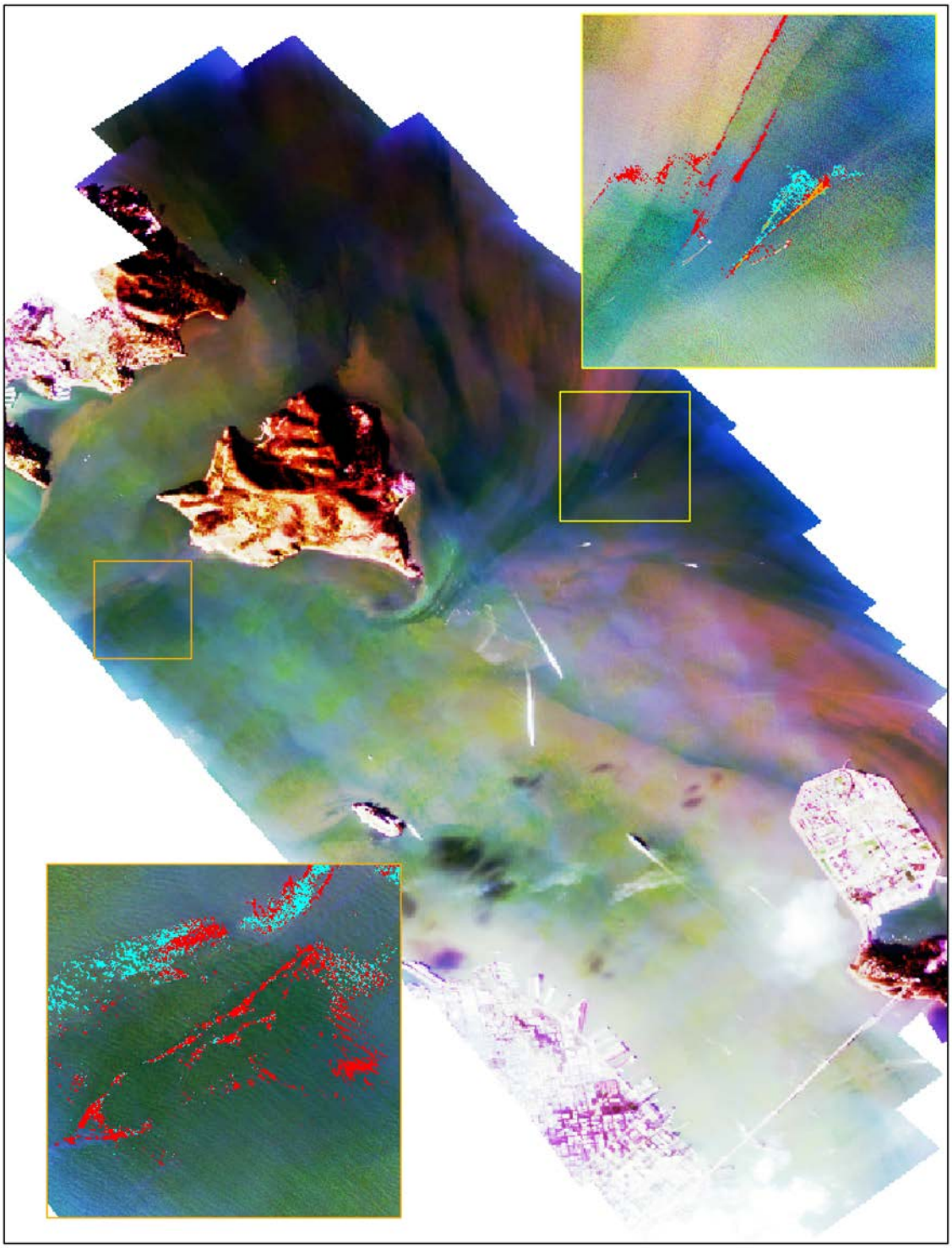

Figure 14. DMSC multispectral mosaic of oil spill area between Tiburon in the north and Oakland Bridge in the south. Insets show samples of derived oil classification.

measurements, we hope to obtain some field data from OSPR and other field recovery crews in the near future for validation.

The flying altitude and hence spatial resolution of the data relative to the size of the existing oil features also partly affected the number of thickness classes that could be reliably extracted from the data. As has been observed in video imagery from other fuel oil spills (e.g. the Prestige spill off Spain) and from our own tests in the Ohmsett tank, heavy fuel oils tend to form slicks with two distinct components – thick oil areas (>0.2mm), and sheen/very thin oil dominated areas (<0.05mm). We believe our algorithm successfully identified and separated these two main components. At greater spatial resolutions more thickness classes could be derived in the thin oil film areas. At 1.7m, however, the different thickness patches and intermittent clear water areas were too spatially averaged out to yield further reliable separation. We also believe that our classification likely underestimated the extents of very thin (silver) sheens due to the high flight altitude, since the increased atmospheric attenuation from water vapor and aerosols masked the weak reflectance variations due to the presence of thin sheens.

Our image acquisition (approximately 30 minutes in length) coincided with a NOAA oil mapping survey done between 12:00 noon and 3pm. The NOAA survey was done visually from a low altitude helicopter. Figure 15 shows the officially released survey map. The NOAA observations of the existence of primarily sheen and strands of thick oil aligned with current fronts generally agree with our classification, however the difference in detail between the visual-based product and our methodology (see Figure 2) is quite obvious.

Our previous algorithm development also allowed the identification of areas with oil that has become emulsified. Figure 16 shows an area in which our choice of imaging wavelengths allowed identification of emulsified oil and its separation from unemulsified oil features. As we reported in our earlier project, prior experiments done over the Santa Barbara oil seeps showed that as emulsification changes the color of the floating oil, it begins to reflect strongly at longer wavelengths while unemulsified oil reflectance tends to be closer to the water background at the same wavelengths. Although we do not have field-validation data at present to prove the existence of emulsified oil in some parts of the scanned region, we feel quite secure in reaching our conclusions based on validated observations in the Santa Barbara Channel.

We are continuing to analyze the collected imagery and test the application of our algorithms. The primary conclusions from this uncommon opportunity are: 1) Our imaging and processing technology can be successfully applied in a real spill situation; 2) The effects of flying altitude on the performance of the algorithms must be considered in conjunction with the spatial distribution characteristics of each spill. For example, the imaging of an illegal bilge dump, or small spill from a moving vessel requires imaging at considerably lower altitude (i.e. higher data resolution) than a massive, coherent, slow moving spill.

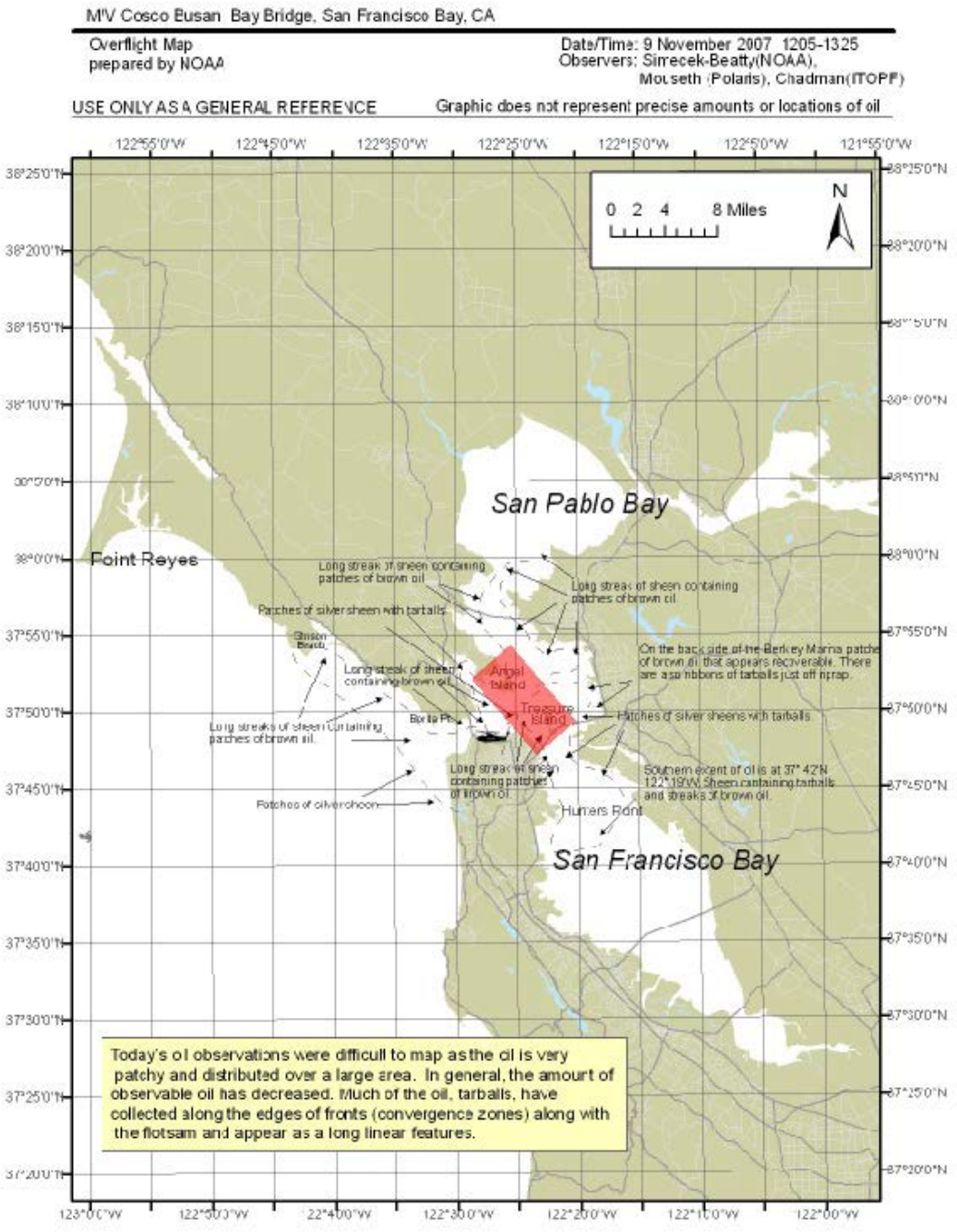

Figure 15. NOAA oil distribution map produced from visual observations during a time interval encompassing our imaging flight. The imaged section is shown in red.

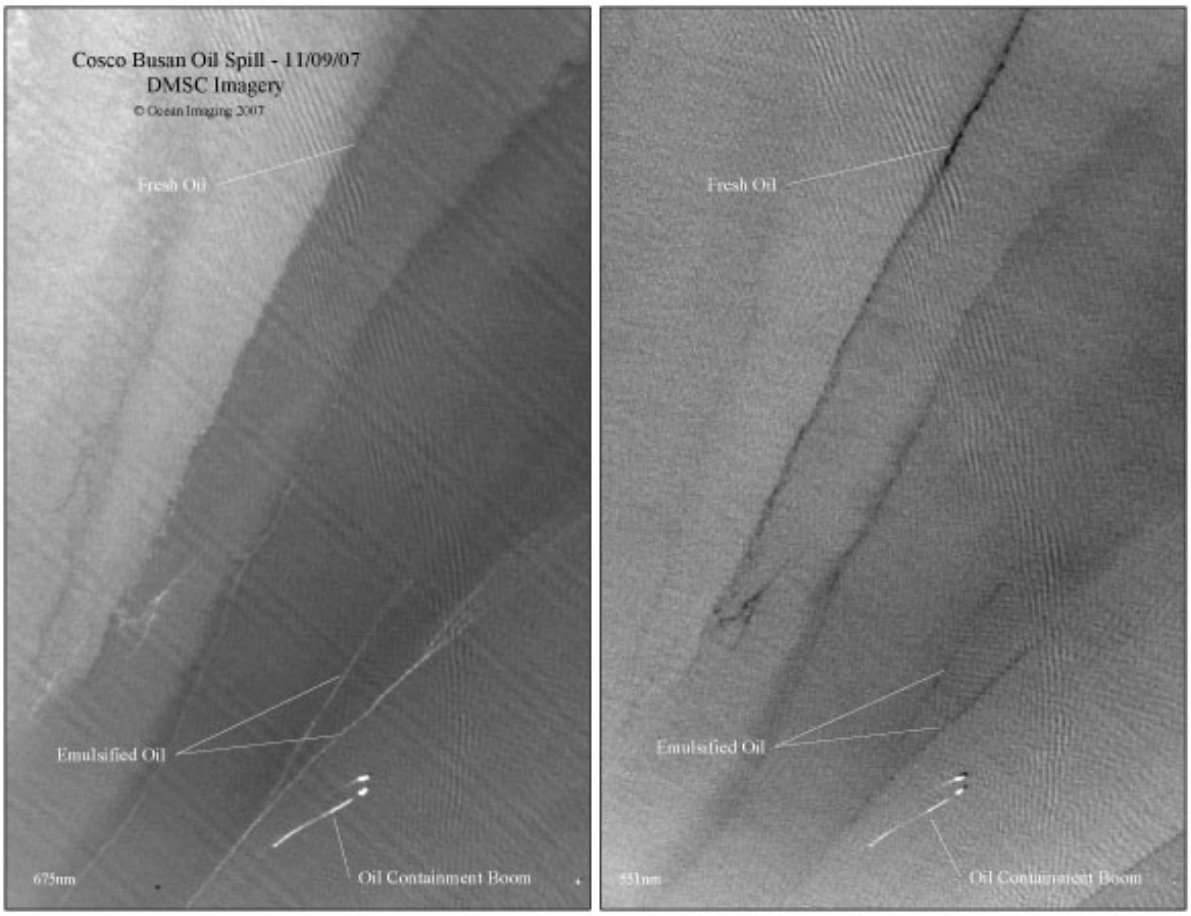

Figure 16. Area of the Bay containing both unemulsified and emulsified oil as imaged by the DMSC at 675nm (left) and 551nm (right). Note how some portions of the slick features exhibit strong reflectance in the 675nm band, indicating emulsification.

3.2 The Platform "A" spill in Santa Barbara Channel.

Early on 12/7/2008 staff working on Platform A in the Santa Barbara channel reported a spill from the platform due to a ruptured hose. The initial spilled volume estimate of 30 gallons was subsequently revised to 1100 – 1400 gallons. The response included aerial overflights by MMS, OSPR and privately chartered helicopter, Clean Seas and other ship deployment, and oil recovery. OSPR requested OI to conduct and overflight with the developed system in late afternoon on 12/8/2008. Image data were collected with the multispectral and IR sensors over the oil spill area. The data were immediately processed and posted on the web-accessible GIS system within 40 minutes of data acquisition, making them available to Central Command for guiding the recovery operations. OI conducted another flight on the morning of 12/10/08 and acquired, processed and

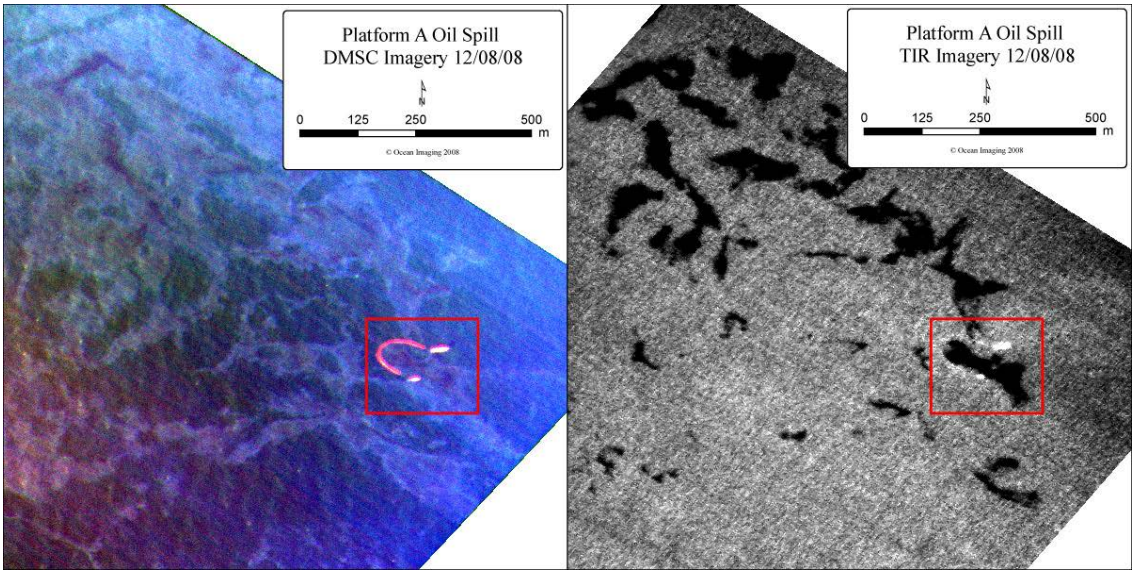

Figure 17. Unclassified multispectral visible (left) and thermal IR (right) imagery of part of the Platform A spill area. In the multispectral image different colors correspond to different oil thicknesses. In the IR data thinner films are not distinguishable but the thickest oil patches show strong contrast. Note the two response vessels surrounding a recoverable thickness oil patch with a containment boom.

disseminated the imagery within 30 minutes of initial data acquisition. The 12/10/08 imaging results showed only small areas of aged and emulsified oil in the general area, which were judged to be residues from natural seepage and not related to the spill. OI also found a small fresh sheen feature offshore which was linked by the responders to a diesel spill from a private vessel. The data supported independent aerial visual surveys that no more recoverable oil from the platform spill was present, and recovery operations were suspended. The 12/8/08 data were subsequently analyzed for total spill volume estimates. Because the imaging activities, thickness classifications and resulting total volume estimates are part of materials used for settlements in this incident, we are not authorized to reproduce detailed results in this public report. We are showing one example in Figure 17, which shows original multispectral imagery and thermal IR imagery of part of the spill area on 12/8/08. Since none of the spilled oil features exceeded the 0.2mm thickness limit, the multispectral data could be used to map oil thicknesses over the entire spill. The IR data were very useful, however, very strongly depicting the locations of the thickest, recoverable oil patches. The IR image in Figure 17 shows two recovery vessels successfully recovering one of these patches.

The use of the developed mapping system was well received by the responders and also received media coverage (e.g. http://www.oceanconserve.org/shared/reader/welcome.aspx?linkid=112837&keybold=oil%20AND%20%20spill%20AND%20%20cleanup).

4. MAJOR PROJECT CONCLUSIONS

The work in this project resulted in the development, demonstration and operational implementation of an aerial oil spill distribution and thickness mapping system. The system is portable, can be duplicated with off the shelf camera and peripheral hardware and requires minimal software customization. The major conclusions reached in this study are:

- Oil-on-water thickness mapping with accuracies useful for operational spill response and post-response assessments is possible using multispectral and IR aerial imagery.

- Oil thickness assessment solely with visible range multispectral data provides a thickness range from silver sheens to approximately 0.15-0.2mm. The addition of a thermal IR camera channel to the multispectral configuration increases the measurement range past 2mm.

- Detection and identification of emulsified vs. unemulsified oil is readily possible.

- The algorithm limitations and image background variability due to different atmospheric haze, sun angle, air/water temperature and other environmental parameters necessitates that the oil thicknesses be binned into thickness range classes (rather than computing a unique absolute thickness for each image pixel). Computations such as total volume are thus represented as a range within defined confidence intervals.

- In operational applications, using the developed GIS technology, it is possible to electronically deliver a final map product to response teams within 1 hr of initial data collection.

- Additional validations, especially during real oil spill situations (vs. controlled lab and tank conditions), should be performed to establish firm accuracy characteristics for the algorithms.

5. FUTURE RESEARCH RECOMMENDATIONS

The work accomplished to-date resulted in the development, testing and initial operational deployment of an aerial oil spill mapping system. The system's algorithms were developed and tested, for logistical reasons, under temperate sea conditions with reasonable water clarity. We recommend that additional testing be done under freezing temperature or arctic conditions which would allow adjustment of the algorithms for use at high latitudes or during winter freeze-up conditions. The response of the thermal IR part of the system for detecting oil under such conditions is of particular interest since, to our knowledge, no such research has yet been done. Additionally, the developed remote sensing methodology should be tested/demonstrated over waters with very high sediment loads that often occur at high latitudes during snowmelt and also along the Gulf of

Mexico coastline. Such tests can serve two important purposes: 1) They will expand the applicability of the developed hardware/software into regions not targeted by the previous work, yet of high importance from offshore oil drilling (and hence oil spill risk) perspective; 2) They will provide a venue for oil spill response groups in those regions to familiarize themselves with the new technology so they can utilize it in future spills. MMS' Ohmsett facility could be utilized for the initial freezing weather/ice conditions work, possibly in conjunction with other research or training that requires ice to be placed in the Ohmsett tank. In-the-field trials could be conducted in Alaskan waters over natural oil seeps. The Gulf of Mexico high turbidity trials can be conducted over natural seeps as well as over existing oil rigs, some of which release small amounts of oil on occasion.

Another follow-on research direction is the adaptation of the developed hardware/software for routine oil rig reconnaissance (versus oil spill response). As the result of this project, we have been approached by companies providing daily oil rig reconnaissance services to oil companies operating unmanned platforms in the Gulf of Mexico. Their interest is in being able to provide more quantitative and spatially accurate documentation than is possible with visual and simple oblique photo observations. We believe a system composed of "downsized" hardware and software components from the one developed for this project would best suite such applications. A single 3-CCD camera system with its channels customized for oil detection would be small enough to be mounted through a modified fuselage inspection port aboard any aircraft (i.e. not requiring a larger, FAA-certified camera port). This will allow widespread use of the new technology by independent operators. Simplified, automated oil thickness classification software would provide sufficient quantitative information while not requiring the operator to be skilled in image processing and GIS. The integration of such a system is relatively simple with existing off-the shelf hardware and it could be field-tested simultaneously with the existing system during the field trials described above.

6. REFERENCES

Byfield, V. 1998. Optical Remote Sensing of Oil in the Marine Environment. PhD Thesis, U. of Southampton, School of Ocean and Earth Science.

Davies L., J. Corps, T. Lunel and K. Dooley. 1999. Estimation of oil thickness. AEA Technology. AEAT-5279(1). 1-34.

Gillot, A., G.H.R. Aston, P. Bonanzinga, Y. le Gal la Salle, M.J. Mason, M.J. O'Neill, J.K. Rudd and D.I. Stonor. 1988. Field guide to application of dispersants to oil spills. Rept No.2/88. The Hague,Netherlands, CONCAWE. 64pp.

Svejkovsky, J. and J. Muskat. 2006. Real-time detection of oil slick thickness patterns with a portable multispectral sensor. Minerals Management Service, Final Report for Project #0105CT39144.

Svejkovsky, J. 2007. Development and evaluation of a cost effective aerial imaging system for oil spill and coastal impact monitoring. Final Report to Calif. Dept. of Fish and Game's Office of Oil spill Prevention and Response, Contract #P0375037.

Svejkovsky, J. 2008. Determination and testing of wavelength combination options for imaging oil-on-water with a UAV. Final Report to Navy-SPAWAR Systems Center, Contract #N66001-08-M-1080

Svejkovsky J., J. Muskat and J. Mullin. 2008. Mapping Oil Spill Thickness with a Portable Multispectral Aerial Imager. Proc. International Oil Spill Conference 2008, 4-8 May, 2008, Savannah, Georgia.